Pressure Gradients of Air and Water/Air Two-Phase Flow in a Stratified Bed

Jin Ho Park, Hyun Sun Park [*], Junghyeon Oh, Mooneon Lee, Moo Hwan Kim
Division of Advanced Nuclear Engineering, POSTECH, Pohang, Gyeoungbuk, Republic of Korea 37673
[*]*Corresponding author: hejsunny@postech.ac.kr*

1. Introduction

In the late phases of a severe accident in a nuclear power plant, assurance of the ex-vessel debris bed coolability is crucial for stabilizing the molten core debris and ultimately terminating severe accident progression. Since this situation causes concrete floor erosion due to molten corium concrete interaction. To achieve this, it is essential to supply sufficient coolant into the internal heat-generating debris bed. The effectiveness of such a coolant supply into a debris bed is determined by the pressure drop through the porous debris bed. For this reason, it is necessary to investigate the pressure drop mechanisms in a debris bed, which is characterized by geometric parameters such as porosity, particle morphology, particle size distribution, and bed stratification. Therefore, among these parameters, the present study focuses on the effect of bed stratification on the pressure gradients in the bed.

2. Models

In order to predict the pressure gradient of a two-phase flow through a debris bed, various analytical models [1-6] have been suggested based on the Ergun equation [7], namely Eq. (1), by including the relative permeabilities and passabilities, with or without consideration of the interfacial drag between liquid and gas. The Ergun equation is a semi-empirical formula for predicting the pressure drop of a single-phase flow in homogeneous beds consisting of mono-sized spherical particles, and is expressed as follows:

$$-\frac{dp}{dz} - \rho_i g = \frac{\mu_i}{K} V_{si} + \frac{\rho_i}{\eta} V_{si}^2$$
$$= \frac{C_1 \mu_i (1-\varepsilon)^2}{\varepsilon^3 d_p^2} V_{si} + \frac{C_2 \rho_i (1-\varepsilon)}{\varepsilon^3 d_p} V_{si}^2 \quad (1)$$

where C_1 and C_2 are the empirical Ergun constants, having values of 150 and 1.75, respectively. Furthermore, μ_i and ρ_i are the dynamic viscosity and density of the i-phase fluid ($i = l$ and g for liquid and gas, respectively), and $-dp/dz$ is the pressure loss through porous media, V_{si}, d_p, and ε are the superficial velocity of a fluid, the particle diameter, and the bed porosity, respectively. The bed porosity is calculated as follows:

$$\varepsilon = 1 - \frac{\sum \left(m_p / \rho_p \right)}{V_t}, \quad (2)$$

where m_p is the mass of particles, ρ_p is the density of the particles, and V_t is the volume of the test section.

The Ergun equation, Eq. (1) can be expressed in a dimensionless form as follows:

$$\frac{-dp/dz - \rho_i g}{\rho_i g} = \psi_i = C_1 \frac{Re_p}{Ga_i} + C_2 \frac{Re_p^2}{Ga_i}, \quad (3)$$

where ψ_i is the dimensionless pressure drop, Re_p is the particle Reynolds number, Eq. (4) and Ga_i is the modified Galileo number, Eq. (5).

$$Re_p = \frac{\rho_i V_{si} d_p}{\mu_i (1-\varepsilon)} \quad (4)$$

$$Ga_i = \left(\frac{\rho_i}{\mu_i} \right)^2 g \left(\frac{d_p \varepsilon}{(1-\varepsilon)} \right)^3 \quad (5)$$

The two-phase flow pressure drop in porous media is expressed by Eqs. (6) and (7) for liquid and gas:

$$-\frac{dp_l}{dz} = \rho_l g + \frac{\mu_l}{K K_{rl}} V_{sl} + \frac{\rho_l}{\eta \eta_{rl}} V_{sl} |V_{sl}| - \frac{F_i}{s} \quad (6)$$

$$-\frac{dp_g}{dz} = \rho_g g + \frac{\mu_g}{K K_{rg}} V_{sg} + \frac{\rho_g}{\eta \eta_{rg}} V_{sg} |V_{sg}| + \frac{F_i}{\alpha} \quad (7)$$

where K_{rl}, K_{rg} and η_{rl}, η_{rg} are the relative permeabilities and passabilties of liquid and gas, respectively. F_i is the interfacial drag between liquid and gas, and s ($= 1 - \alpha$) is liquid saturation.

Table I shows relative permeabilities and passabilities in the models without consideration of the interfacial friction, and the relative permeabilities, passabilities, and the interfacial frictions of the models considering interfacial friction, explicitly are listed in Table II – IV.

Table I: Relative permeabilities and passabilities in the models without consideration of the interfacial friction

	K_{rg}	η_{rg}	K_{rl}	η_{rl}	F_i
Reed [1]	α^3	α^5	s^3	s^5	-
Lipinski [2]	α^3	α^3	s^3	s^3	-
Hu and Theofanous [3]	α^3	α^6	s^3	s^6	-

Table II: Relative permeabilities, passabilities and the interfacial friction in Schulenberg and Müller model

	K_{rg}	η_{rg}	K_{rl}	η_{rl}
Schulenberg and Müller [4]	α^3	$0.1\alpha^4 \ (\alpha \leq 0.3)$ $\alpha^6 \ (\alpha > 0.3)$	s^3	s^5
[*] $F_i : 350 s^7 \alpha \dfrac{\rho_l K}{\eta \sigma} (\rho_l - \rho_g) g V_r^2$				

As a result of visualization in water/air flow experiments, Tung and Dhir [5] defined flow regimes. In Table III, α_1 is defined by the minimum value between 0.3 and $0.6(1 - \gamma)^2$ where γ is the ratio of the bubble diameter D_b, Eq. (8) and the particle diameter d_p,

$$D_b = 1.35 \sqrt{\frac{\sigma}{g(\rho_l - \rho_g)}} \quad (8)$$

$\alpha_2 = \pi/6 \approx 0.52$, $\alpha_3 = 0.6$, and $\alpha_4 = \pi\sqrt{2}/6 \approx 0.74$. The interfacial frictions and its coefficients according to the flow regime are listed in Table IV. In here, the relative velocity V_r and the geometric factor f are defined by Eqs. (9) and (10), respectively. For smooth transition between flow regimes, the weighting function was defined and more specific information is in their paper [5].

$$V_r = \frac{V_{sg}}{\alpha} - \frac{V_{sl}}{s} \tag{9}$$

$$f = \frac{1}{2}(1+\gamma)\ln(1+\frac{2}{\gamma}) \tag{10}$$

Table III: Relative permeabilities and passabilities according to flow regime in Tung and Dhir model [5]

	Flow regime	K_{rg}	η_{rg}	K_{rl}	η_{rl}
α_1	Bubbly	$(\frac{1-\varepsilon}{1-\varepsilon\alpha})^{4/3}\alpha^4$	$(\frac{1-\varepsilon}{1-\varepsilon\alpha})^{2/3}\alpha^4$		
	Transition	-	-		
α_2					
	Slug	$(\frac{1-\varepsilon}{1-\varepsilon\alpha})^{4/3}\alpha^4$	$(\frac{1-\varepsilon}{1-\varepsilon\alpha})^{2/3}\alpha^4$	s^4	s^4
α_3					
	Transition	-	-		
α_4	Annular	$(\frac{1-\varepsilon}{1-\varepsilon\alpha})^{4/3}\alpha^3$	$(\frac{1-\varepsilon}{1-\varepsilon\alpha})^{2/3}\alpha^3$		

Table IV: The interfacial frictions and the coefficients according to flow regime in Tung and Dhir model [5]

$(0 < \alpha < \alpha_1)$ Bubbly: $C_v = 18\alpha f, C_i = 0.34 s^3 \alpha f^2$
$F_i = C_v \frac{\mu_l}{D_b^2 \varepsilon} s V_r + C_i \frac{(s\rho_l + \alpha\rho_g)}{D_b \varepsilon^2} s^2 V_r |V_r|$
$(\alpha_1 < \alpha < \alpha_2)$ Transition
$(\alpha_2 < \alpha < \alpha_3)$ Slug: $C_v = 5.21\alpha, C_i = 0.92 s^3 \alpha$
$F_i = C_v \frac{\mu_l}{D_b^2 \varepsilon} s V_r + C_i \frac{(s\rho_l + \alpha\rho_g)}{D_b \varepsilon^2} s^2 V_r |V_r|$
$(\alpha_3 < \alpha < \alpha_4)$ Transition
$(\alpha_4 < \alpha < 1)$ Annular
$F_i = \frac{\mu_g}{KK_{rg}} s\alpha V_r + \frac{\rho_g}{\eta\eta_{rg}} s\alpha^2 V_r |V_r|$

Schmidt [6] modified the Tung and Dhir model [5] in order to consider small particle sizes. First, the bubble diameter was defined based on the minimum value between the bubble diameter suggested by Tung and Dhir [5] shown in Eq. (8) and $(\sqrt{2}-1)d_p$. Second, the void fractions for the flow pattern boundaries were defined as indicated in Table V. Third, a multiplicative factor $(d_p/6 \text{ mm})^2$ was proposed for particles smaller than 6 mm, and an additional multiplier $(1-\alpha)^2$ was also proposed for the annular flow regime to obtain a more realistic decrease of the interfacial drag for increasing void fraction. Thus, Schmidt [6] suggested using the interfacial drag between liquid and gas for annular flow as follows:

$$F_i = \left(\frac{\mu_g}{KK_{rg}} s\alpha V_r + \frac{\rho_g}{\eta\eta_{rg}} s\alpha^2 V_r |V_r| \right) \times (1-\alpha)^2 \min\left(1, \left(\frac{d_p}{6mm} \right)^2 \right) \tag{11}$$

Table V. Void fractions for flow pattern boundaries

	Schmidt [6]
α_1	$\frac{\pi/6}{5}(d_p - 0.008) + \alpha_{1,TD}$ $(d_p < 8mm)$ $\alpha_{1,TD}$ $(d_p > 8mm)$
α_2	$\frac{\pi/6}{5}(d_p - 0.008) + \alpha_{2,TD}$ $(d_p < 8mm)$ $\alpha_{2,TD}$ $(d_p > 8mm)$
α_3	$\frac{\pi/6}{5}(d_p - 0.008) + \alpha_{3,TD}$ $(d_p < 8mm)$ $\alpha_{3,TD}$ $(d_p > 8mm)$
α_4	$\frac{\pi/6}{5}(d_p - 0.006) + \alpha_{4,TD}$ $(d_p < 6mm)$ $\alpha_{4,TD}$ $(d_p > 6mm)$

Nevertheless, the models still have uncertainties in the evaluation of the resulting cooling potential of an ex-vessel debris bed due to the complexity of the bed structure, the interactions among the phases, and the influence of flow patterns on pressure drop, especially in the debris bed composed of small size particles less than or equal to 5 mm. Thus, our previous study [8] proposed a new improved model for prediction of the two-phase flow pressure drop through porous media. The adequacy of the proposed model was verified by comparison with various existing experimental data [9-11] for particle diameters of 3.18 – 6.35 mm.

A new improved model for two-phase flow pressure drop in porous media [8] was developed with three modifications based on Schmidt model [6]. The first modification is the replacement of the new Ergun constants ($C_1 = 36k_0\tau^2$ and $C_2 = 3\tau(3/2 + 1/\beta^4 - 5/2\beta^2)/4$) instead of the existing Ergun constants [12]. The second modification is an increase in the additional multiplier for the interfacial drag in the annular flow regime F_i proposed by Schmidt [6], from $(1-\alpha)^2$ in Eq. (11) to $(1-\alpha)^4$. Lastly, the third modification is to change the exponents of relative permeability and relative passability for liquid from $K_{rl} = s^4$ and $\eta_{rl} = s^4$ to $K_{rl} = s^3$ and $\eta_{rl} = s^5$.

To consider the effect of particle size distribution on pressure gradients in porous media, various mean particle diameters (mass d_m, area d_a, length d_l, and number d_n) have been suggested as the effective diameter. The suggested mean diameters for multi size particles are defined as Eqs. (12) – (15). Where d_j is the particle size, f_j is the fraction of the number of particles in the bed.

$$d_m = \sum d_j m_j = \sum \left(d_j \frac{d_j^3 f_j}{\sum d_j^3 f_j} \right) \qquad (12)$$

$$d_a = \sum d_j a_j = \sum \left(d_j \frac{d_j^2 f_j}{\sum d_j^2 f_j} \right) \qquad (13)$$

$$d_l = \sum d_j l_j = \sum \left(d_j \frac{d_j f_j}{\sum d_j f_j} \right) \qquad (14)$$

$$d_n = \sum d_j n_j = \sum \left(d_j \frac{f_j}{\sum f_j} \right) \qquad (15)$$

3. Experiment

3.1 Experimental Facility with Measurement System

To conduct a series of experiments for measuring the pressure drop of air and water/air two-phase flow through a stratified bed under isothermal conditions (20°C, 1 bar) varying the gas flow rates, an experimental facility called PICASSO (Pressure drop Investigation and Coolability ASSessment through Observation) as shown in Fig. 1 was used. A detailed description on PICASSO and measurement system can be found in our previous study [13].
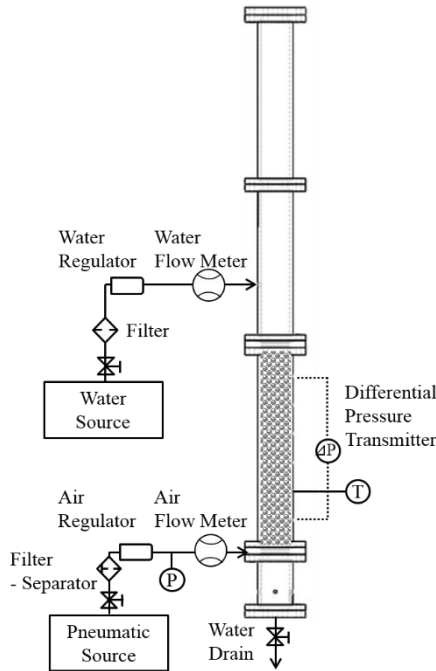
Fig. 1. Schematic of the PICASSO experimental facility.

3.2 Experimental Bed and Procedure

The properties of a stratified bed are listed in Table VI. In this experimental case, 5 mm spherical particles were loaded as the lower half of the test section (365 mm and ε: 0.383), while 2 mm spherical particles were stacked thereon (370 mm and ε: 0.391) with mass ratio of 1:1.

The total bed porosity is 0.387, and various mean particle diameters are calculated by using Eqs. (12) – (15).

Table VI: Properties of a stratified bed

Exp. case	ε	d_m (mm)	d_a (mm)	d_l (mm)	d_n (mm)
PCS-SSB1	0.387	3.50	2.86	2.41	2.18

The experimental procedure is as in the following. At the beginning of the experiment, the total mass of particles in each size (2 and 5 mm) is measured to obtain the bed porosity, and then the particles are packed in the test section. Second, the pressure impulse lines are filled with the single-phase fluid (the air for single-phase air experiment or the water for water/air two-phase experiment). Third, the upward air is injected from the bottom of the bed, and the air flow rate and the pressure gradients are measured by data acquisition system when steady-state condition is established. Finally, the air flow rate is changed to another value, and immediately above step is repeated from 3 to 350 L/min.

4. Experimental Results and Discussion

4.1 Pressure Gradients of Air Flow in a Stratified Bed

Fig. 2 provides a comparison between the measured pressure gradients of air flow through the stratified bed, expressed in four forms (d_m, d_a, d_l, and d_n), and values predicted by the proposed model [12]. The experimental data in PCS-SSB1 agrees with the values predicted by the proposed model [12] within a mean absolute percentage deviation of 5% when adopting the area mean diameter d_a as the effective diameter. Furthermore, the experimental data adopting d_m, d_l, and d_n have mean absolute percentage deviations of 27%, 32%, and 56%, respectively, relative to the values predicted by the proposed model. Therefore, it is appropriate to apply the area mean diameter as the effective diameter for predicting the pressure drop of air flow in a stratified bed.
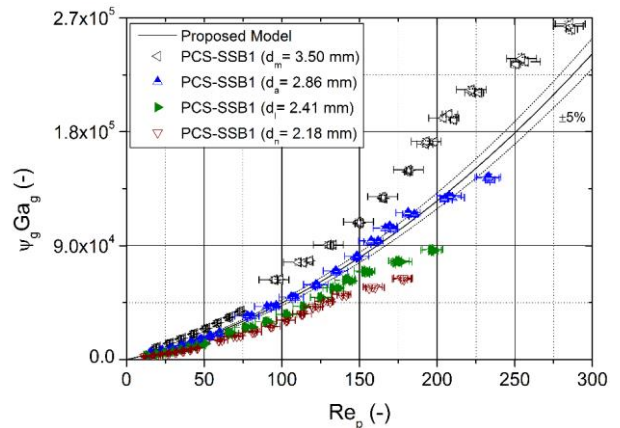
Fig. 2. Dimensionless pressure gradients of air flow in stratified bed (PCS-SSB1), composed of spherical particles (2 and 5 mm) with mass ratio of 1:1 (solid line: values predicted by proposed model, short dot lines: ±5% error of predicted values).

4.2 Pressure Gradients of Water/Air Two-Phase Flow in a Stratified Bed

Fig. 3 shows the dimensionless pressure gradients of the water/air flow in PCS-SSB1 without additional water inflow. The error bars represent the instrument nominal accuracy, and the curves represent the values predicted by the proposed model [8], adopting mean particle diameters. It is notable that the dimensionless pressure gradients of the water/air flow in PCS-SSB1 decrease above the superficial air velocity of 0.17 m/s without reaching the hydrostatic pressure gradient $(-dp/dz)^* = 1$. It is conjectured that this is because the flow regime in the upper part of the bed (2 mm sphere) and that in lower part (5 mm sphere) are different, although the void fraction is the same due to the steady-state condition.

A comparison between the measured pressure gradients of the water/air flow in PCS-SSB1 and values predicted by the proposed model adopting mean particle diameters demonstrates that it is difficult to apply the results obtained from the air flow experiment (the area mean diameter is appropriate as the effective diameter) to the water/air two-phase flow. However, it can be seen that the proposed model (solid red line) can predict the experimental data by averaging the predicted values according to the bed height after calculating the upper part (2 mm sphere, bed height: 370 mm and ε: 0.391) and lower part (5 mm sphere, bed height: 365 mm and ε: 0.383) of the bed. This can be expressed as follows:

$$\text{Predicted value in the upper (2 mm)} \times \frac{370}{735}$$
$$+\text{Predicted value in the lower (5 mm)} \times \frac{365}{735} \quad (16)$$
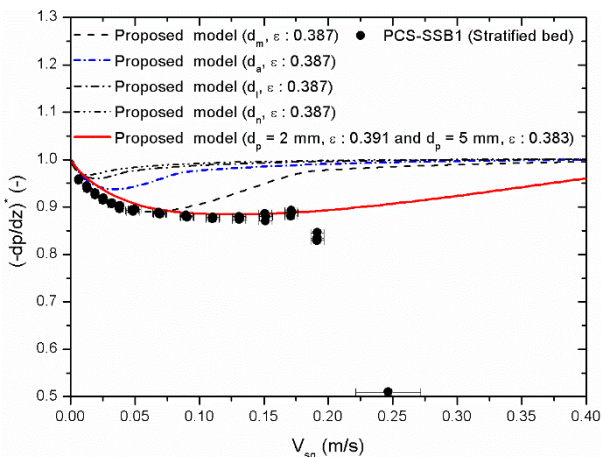
Fig. 3. Dimensionless pressure gradients of water/air flow in PCS-SSB1 with no additional water inflow, and values predicted by proposed model adopting mean diameters.

5. Conclusions

Through the experimental results, the pressure gradients of air flow in a stratified bed predicted by the proposed model from previous study [12] within a mean absolute percentage deviation of 5% when adopting the area mean diameter d_a as the effective diameter.

A comparison between the measured pressure gradients of the water/air two-phase flow in a stratified bed and values predicted by the proposed model [8] demonstrated that it is difficult to verify whether the area mean diameter d_a is appropriate as the effective diameter. Instead, the proposed model [8] predicted the experimental data by means of averaging according to the bed height after calculating the upper and lower parts of the bed.

REFERENCES

[1] Reed, A.W., The effect of channeling on the dryout of heated particulate beds immersed in a liquid pool. 1982, Massachusetts Institute of Technology.
[2] Lipinski, R.J., Model for boiling and dryout in particle beds. [LMFBR]. 1982. p. Medium: X; Size: Pages: 177.
[3] Hu, K. and T. Theofanous, On the measurement and mechanism of dryout in volumetrically heated coarse particle beds. International journal of multiphase flow, 1991. 17(4): p. 519-532.
[4] Schulenberg, T. and U. Müller, An improved model for two-phase flow through beds of coarse particles. International journal of multiphase flow, 1987. 13(1): p. 87-97.
[5] Tung, V. and V. Dhir, A hydrodynamic model for two-phase flow through porous media. International journal of multiphase flow, 1988. 14(1): p. 47-65.
[6] Schmidt, W., Influence of multidimensionality and interfacial friction on the coolability of fragmented corium. 2004.
[7] Ergun, S., Fluid flow through packed columns. Chem. Eng. Prog., 1952. 48: p. 89-94.
[8] Park, J.H., et al., Modeling of Pressure Drop in Two-Phase Flow of Mono-Sized Spherical Particle Beds. International Journal of Heat and Mass Transfer, 2018. To be published.
[9] Tutu, N., T. Ginsberg, and J. Chen, Interfacial drag for two-phase flow through high permeability porous beds. Journal of heat transfer, 1984. 106(4): p. 865-870.
[10] Chikhi, N., et al., Pressure drop and average void fraction measurements for two-phase flow through highly permeable porous media. Annals of Nuclear Energy, 2016. 94: p. 422-432.
[11] Li, L., et al., Pressure losses and interfacial drag for two-phase flow in porous beds with coarse particles. Annals of Nuclear Energy, 2017. 101: p. 481-488.
[12] Park, J.H., et al., Influence of Particle Morphology on Pressure Gradients of Single-Phase Air Flow in the Mono-Size Non-Spherical Particle Beds. Annals of Nuclear Energy, 2018. 115: p. 1-8.
[13] Park, J.H., et al., Adequacy of effective diameter in predicting pressure gradients of air flow through packed beds with particle size distribution. Annals of Nuclear Energy, 2018. 112: p. 769-778.